frontiers | Frontiers in Astronomy and Space Sciences

TYPE Review
PUBLISHED 06 August 2024
DOI 10.3389/fspas.2024.1436202

OPEN ACCESS

EDITED BY
Pedro Sarriguren,
Spanish National Research Council (CSIC), Spain

REVIEWED BY
Praveen C. Srivastava,
Indian Institute of Technology Roorkee, India
Myung-Ki Cheoun,
Soongsil University, Republic of Korea

*CORRESPONDENCE
Gianluca Colò,
colo@mi.infn.it

RECEIVED 21 May 2024
ACCEPTED 20 June 2024
PUBLISHED 06 August 2024

CITATION
Colò G and Niu Y (2024), Quasi-particle–vibration coupling approach for nuclear β-decay.
Front. Astron. Space Sci. 11:1436202.
doi: 10.3389/fspas.2024.1436202

Quasi-particle–vibration coupling approach for nuclear β-decay

Gianluca Colò [1,2]* and Yifei Niu [3,4]

[1]Dipartimento di Fisica "Aldo Pontremoli", Università degli Studi, Milano, Italy, [2]INFN, Sez. di Milano, Milano, Italy, [3]School of Nuclear Science and Technology, Lanzhou University, Lanzhou, China, [4]Frontiers Science Center for Rare Isotope, Lanzhou University, Lanzhou, China

The study of β-decay is important to answer open questions in physics and astrophysics; however, theoretical predictions of the associated half-lives are still plagued by uncertainties. In this short review, we argue that a reliable model for this study is nuclear density functional theory (DFT), complemented by further specific correlations; the quasi-particle–vibration coupling (QPVC) model has been successful in predicting half-lives in a number of spherical nuclei, and its extension to deformed systems should be envisioned. Some remaining open questions are addressed.

KEYWORDS

nuclear density functional theory, quasi-particle–vibration coupling, Skyrme effective interactions, Gamow–Teller transitions, pairing in nuclei

1 Introduction

The β-decay of atomic nuclei is a fundamental process that is studied both with the goal of understanding the nuclear many-body problem and because of the role it plays in several contexts, like astrophysics and particle physics (Rubio et al., 2020). The synthesis of the elements observed in the Universe at different scales is one of the major unsolved problems in physics, and if we consider medium-heavy elements beyond the iron region, they are formed as the result (mainly) of the competition between neutron capture and β-decay; thus, either measured or theoretically calculated β-decay rates are a mandatory ingredient for the understanding of nucleosynthesis (Langanke and Martínez-Pinedo, 2003; Qian and Wasserburg, 2007; Kajino et al., 2019). The inverse process, electron capture by nuclei, governs instead the supernova explosion, together with the neutrino mean free path (Janka et al., 2016). Therefore, not only β-decay but also all electroweak processes involving nuclei should be amenable to a reliable, systematic description when tackling the big questions related to astrophysics and cosmology. Moving to particle physics, although the standard model is inherently "vector minus axial" in the weak sector, the search for other couplings is a very active field of research [a recent review on new questions and opportunities is presented by Hayen (2024)]. Among the tensions and puzzles of the standard model, we can single out the lack of unitarity of the Cabibbo–Kobayashi–Maskawa (CKM) matrix and the hierarchy of the neutrino masses. Superallowed β-decay and its precision measurement are the way to pin down the CKM matrix element $V_{\rm ud}$ (Gorchtein and Seng, 2024). Finally, a reliable description of single β-decay is a preliminary step for being confident to attack the more complicated two-step process, that is, neutrinoless $\beta\beta$-decay; this is the avenue to access the still unknown hierarchy of neutrino masses (Dolinski et al., 2019).

One of the reasons why many basic questions like those mentioned above are still unanswered is the lack of a full understanding of the nuclear single β-decay. It is well known that we still do not have a nuclear "standard model" that allows systematic estimates of observables like the β-decay half-life with controlled theoretical uncertainties. *Ab initio* calculations, despite the claim of being able to explain the quenching of the coupling constant that is responsible for β-decay (Gysbers et al., 2019), cannot treat medium-heavy nuclei. A realistic shell model can achieve a successful description of several half-lives but also has limitations and cannot access the whole isotope chart. Currently, nuclear density functional theory (DFT) (Schunck, 2019; Colò, 2020) is the only microscopic model that is capable of treating all nuclei throughout the isotope chart. The purpose of this mini-review is to demonstrate that DFT, with the inclusion of further correlations, can achieve a parameter-free description of nuclear β-decay.

2 Nuclear structure and β-decay

Even single-β-decay, let alone other weak processes like double-β decay, constitutes a significant challenge for the nuclear structure. We can explain it in simple terms by using the neutron-rich ^{132}Sn isotope as an example. This nucleus undergoes β^- decay, in which

$$(N,Z) \to (N-1,Z+1) + e^- + \bar{\nu}_e, \tag{1}$$

(we will use the standard nomenclature of "parent" and "daughter" nuclei in what follows). The half-life $t_{1/2}$ of a process like Eq. 1 is given by the formula

$$t_{1/2} = \frac{D}{g_V^2 f B_{\mathrm{F}} + g_A^2 f B_{\mathrm{GT}}}, \tag{2}$$

where D = 6,163.4 s and the denominator includes Fermi (F) transitions and Gamow–Teller (GT) transitions. Sometimes, a non-negligible contribution from higher-order transitions (like first-forbidden transitions) should also be included. g_V and g_A are the vector and axial coupling constants, respectively, while the elements B of the reduced transition matrix are given by

$$B_{\mathrm{O}} = \frac{|\langle f||O||i\rangle|^2}{2J_i+1}, \tag{3}$$

where O represents the operator (F, GT, etc.) and i (f) labels the initial (final) states in the parent (daughter) nuclei. In Eq. 2, the phase space factor f is also involved with B taken from Eq. 3.

Strictly speaking, Eq. 2 is valid for the one discrete F and GT state. There may be a set of discrete states or, if one goes above the particle threshold, a continuum distribution of strength. By restricting ourselves to the GT case and labeling with the integral symbol, the sum over discrete states or the integral over a continuum GT distribution $B_{\mathrm{GT}}(E)$, Eq. 2 becomes

$$t_{1/2} = \frac{D}{g_A^2 \int_0^{Q_\beta} dE\, f(\omega)\, B_{\mathrm{GT}}(E)}. \tag{4}$$

Energy conservation dictates the decay is possible when the decay Q-value, Q_β, is positive. In the case of the decay to the ground state of the daughter nucleus, the energies carried away by the electron and (anti)-neutrino are equal to Q_β. If the nucleus decays over an excited state at energy E, the energies carried away by the leptons are smaller, and clearly, E cannot exceed Q_β (in the usual jargon, it lies in the β-decay window or Q_β window). This explains the integration limits in Eq. 4. Another important point is that the phase space factor f is written in Eq. 4 as a function of $\omega = Q_\beta + m_e c^2 - E$, which is the electron kinetic endpoint and is easy to determine experimentally; this function is

$$f(\omega) = \int_{m_e c^2}^{\omega} dE_e\, p_e E_e (\omega - E_e)^2 F(Z+1, E_e), \tag{5}$$

with the electron energy, momentum, and Fermi function denoted as E_e, p_E, and F, respectively. These facts have two important consequences. If, in a theoretical calculation, there is no strength, or very little strength, below Q_β, then the decay half-life is infinite or largely overestimated. However, the position of the final states within the Q_β window is also very important. If the states have lower energies E, $f(\omega)$ increases significantly, and the half-life is, consequently, very sensitive to the values of the final state energies. This explains why β-decay is a challenge for nuclear structure models: it calls for high accuracy in calculations of the low-lying spectra of the daughter nucleus because of the "magnifying lens" effect of the phase space factor.

Figure 1 (the left panel) shows possible GT transitions in the nucleus presented as an example for our general discussion, i.e., ^{132}Sn. There are many single-particle transitions, but, as is well known, most of their GT strength will be absorbed by the collective Gamow–Teller resonance (GTR) at higher energy, 16.3 MeV, in the daughter nucleus ^{132}Sb (in other words, outside the Q_β window, that is 3.089 MeV). This is the result of the strong (spin–isospin) residual force that couples single-particle transitions; this effect and the resulting GT resonance are depicted in the right panel of Figure 1. The GT resonance has been recently measured (Yasuda et al., 2018). In this experiment, the strength up to 25 MeV exhausts ≈ 60% of the appropriate sum rule, that is, the Ikeda sum rule $3(N-Z)$. In the Q_β window, two states are experimentally known at 1.325 MeV and 2.268 MeV, respectively (Mach et al., 1995). The lowest state exhausts 99% of the decay rate.

In the next section, we discuss the capability of our theoretical model to account for this picture in ^{132}Sn and other nuclei. The (quasi-particle) random phase approximation (QRPA) can account for the formation of the GTR but not necessarily for the overall strength distribution as it tends to neglect the spreading and fragmentation of such strength. We shall introduce our model (QRPA + QPVC) and explain how it can account for such fragmentation and increase the strength (also) in the Q_β window. The right panel of Figure 1 presents a simple picture of these findings.

3 Theory

Calculations of the low-lying GT states, starting from an even–even parent nucleus, can be performed within DFT using the linear response theory. We should stress that this approach is parameter-free, although the results can be sensitive to the choice of the energy density functional (EDF), which is not unique. In this

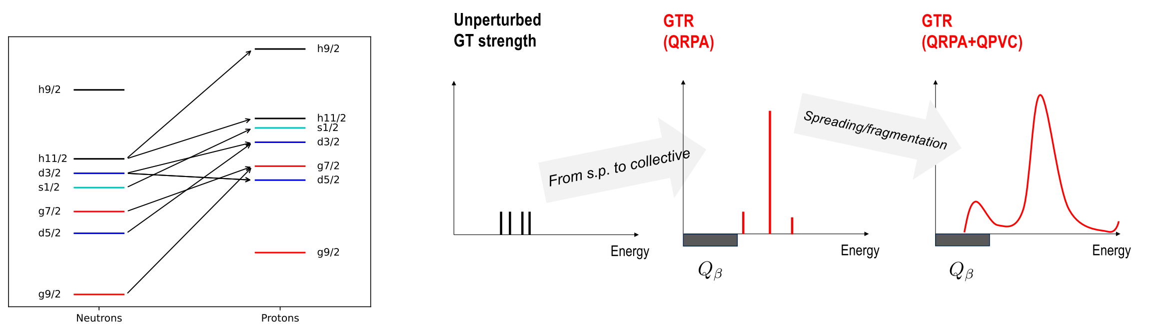

FIGURE 1
(Left panel) Schematic view of the neutron and proton levels, with the possible GT transitions between occupied neutron levels and unoccupied proton levels for ^{132}Sn. The figure is inspired by Figure 8 in the study by Rubio et al. (2020). (Right panel) Schematic view of the different approximations used to calculate the $B(GT)$ distributions. The different GT transitions between occupied and unoccupied levels merge to a large extent into the collective GTR (the residual interaction is repulsive in this case, and the GTR lies at higher energy than the average of the s.p. transitions). QRPA plus QPVC produces a downward shift in strength and significant fragmentation: this increases the likelihood of finding a realistic amount of strength within the Q_β window.

contribution, we discuss the results obtained by using local (i.e., Skyrme) EDFs.

The ground state of an even–even nucleus is obtained by minimizing the total energy, $E = \int d^3r\, \mathcal{E}$, where $\mathcal{E}$ is the EDF, subject to the constraints of a given proton and neutron number. In principle, one could also impose a given deformation as a constraint; however, we only discuss spherical nuclei in this paper. This minimization process involves solving the Hartree–Fock–Bogoliubov (HFB) equations, which can be reduced to HF when pairing vanishes and the nucleus is not superfluid. In this context, the linear-response theory mentioned earlier is the well-known (quasi-particle) QRPA. Within QRPA, an excited state is described as a linear superposition of two quasi-particle (2qp) excitations that become particle-hole excitations when pairing is absent. If α ($\alpha^\dagger$) label the annihilation (creation) operator for quasi-particles, the QRPA eigenstates $|n\rangle$ are created by the operator $\Gamma_n^\dagger$ acting on the ground state, $\Gamma_n^\dagger|0\rangle$. This creation operator is given by

$$\Gamma_n^\dagger = \sum_{\pi\nu} X_{\pi\nu}^{(n)} \alpha_\pi^\dagger \alpha_\nu^\dagger - Y_{\pi\nu}^{(n)} \alpha_\nu \alpha_\pi, \tag{6}$$

where X and Y are the amplitudes to be determined. The notation of Eq. 6 makes it clear that, in this case, we study GT or other multipole excitations that are superposition of *proton–neutron* excitations. This so-called *charge-exchange* version of QRPA describes excitations in the nuclei $(N \mp 1, Z \pm 1)$: both types of excitations are present in the QRPA basis. However, the QRPA eigenstates can be shown to have T_z as a good quantum number, ensuring that the states in the two possible final nuclei can be distinguished. The QRPA eigenstates satisfy the equation

$$\begin{pmatrix} A_{\pi\nu,\pi'\nu'} & B_{\pi\nu,\pi'\nu'} \\ -B^*_{\pi\nu,\pi'\nu'} & -A^*_{\pi\nu,\pi'\nu'} \end{pmatrix} \begin{pmatrix} X_{\pi\nu}^{(n)} \\ Y_{\pi\nu}^{(n)} \end{pmatrix} = E_n \begin{pmatrix} X_{\pi\nu}^{(n)} \\ Y_{\pi\nu}^{(n)} \end{pmatrix}, \tag{7}$$

which is an eigenvalue equation in the matrix form.

Our formalism for charge-exchange RPA and QRPA on top of BCS was introduced by Fracasso and Colò (2007) [see also Colò et al. (2013) and the web page `ns4exp.mi.infn.it` that is part of the `Theo4Exp` platform developed under the EURO-LABS project implemented with the Horizon Europe in program]. We extended this formalism to HFB plus QRPA by Niu et al. (2016), and we refer to this work for details on the above formulas. Other groups have developed charge-exchange QRPA and applied it to the study of β-decay. Many works include, at least in part, phenomenological ingredients (Homma et al., 1996; Möller et al., 1997; Borzov, 2006; Fang et al., 2013). Focusing on microscopic approaches (Nikšić et al., 2005; Marketin et al., 2012; Niu et al., 2013; Mustonen and Engel, 2016; Shafer et al., 2016; Ney et al., 2020), QRPA tends to overestimate half-lives precisely for the reasons that we alluded to previously. QRPA allows the p-h or 2qp configurations to interact so that the GTR can develop; however, it does not necessarily account for the overall fragmentation of the GT strength, so at times, the low-lying strength in the Q_β window is absent or little.

To remedy this shortcoming, we proposed to extend QRPA to QRPA plus quasi-particle–vibration coupling (QRPA plus QPVC). In it, we go beyond the QRPA "linear" assumption, and we propose a more general *ansatz* for the excited states that we now label by $|N\rangle$. Within this ansatz, we include the coupling of the QRPA two quasi-particle states with so-called "doorway states," made with two quasi-particles plus one extra QRPA phonon. Next, we describe the basics of QRPA plus QPVC so that the reader can understand it and have enough background to look at the results presented. We skip some details of the model; for those, we refer to Niu et al. (2016), where the model is discussed more extensively.

In formal terms, the QRPA + QPVC eigenstates $|N\rangle$ are created by the operator $\mathcal{O}_N^\dagger$ acting on the ground state, where

$$\mathcal{O}_N^\dagger = \sum_{\pi\nu} X_{\pi\nu}^{(N,1)} \alpha_\pi^\dagger \alpha_\nu^\dagger - Y_{\pi\nu}^{(N,1)} \alpha_\nu \alpha_\pi + \sum_{\pi\nu;n} X_{\pi\nu;n}^{(N,2)} \alpha_\pi^\dagger \alpha_\nu^\dagger \Gamma_n^\dagger - Y_{\pi\nu;n}^{(N,2)} \Gamma_n \alpha_\nu \alpha_\pi. \tag{8}$$

The first two terms in this latter equation are the same as in QRPA [see Eq. 6], while the last two terms take into account coupling with the doorway states. In principle, one should solve the equation of motion for this new operator with the same technique that is used in standard QRPA. This means that one should solve

$$\langle \mathrm{QPVC}| \left[\delta\mathcal{O}_N, \left[H, \mathcal{O}_N^\dagger\right]\right] |\mathrm{QPVC}\rangle = E_N \langle \mathrm{QPVC}| \left[\delta\mathcal{O}_N, \mathcal{O}_N^\dagger\right] |\mathrm{QPVC}\rangle. \quad (9)$$

Here, E_N is the excitation energy with respect to the ground state $|\mathrm{QPVC}\rangle$, which is now defined as the vacuum of the QPVC annihilation operators $\mathcal{O}_N$. Eq. 9 provides the full QPVC equations that are similar to those of second RPA (Yannouleas, 1987) and can be cast in matrix form as

$$\begin{pmatrix} A_{\pi\nu,\pi'\nu'} & B_{\pi\nu,\pi'\nu'} & A_{\pi\nu,\pi'\nu'n'} & 0 \\ -B^*_{\pi\nu,\pi'\nu'} & -A^*_{\pi\nu,\pi'\nu'} & 0 & -A^*_{\pi\nu,\pi'\nu'n'} \\ A_{\pi\nu n,\pi'\nu'} & 0 & A_{\pi\nu n,\pi'\nu'n'} & 0 \\ 0 & -A^*_{\pi\nu n,\pi'\nu'n'} & 0 & -A^*_{\pi\nu n,\pi'\nu'n'} \end{pmatrix} \begin{pmatrix} X_{\pi'\nu'} \\ Y_{\pi'\nu'} \\ X_{\pi'\nu'n'} \\ Y_{\pi'\nu'n'} \end{pmatrix} = E_N \begin{pmatrix} X_{\pi'\nu'} \\ Y_{\pi'\nu'} \\ X_{\pi'\nu'n'} \\ Y_{\pi'\nu'n'} \end{pmatrix}, \quad (10)$$

where the labels $(N,1)$ and $(N,2)$ of the X and Y amplitudes have been omitted for simplicity. In principle, the new eigenstates $|N\rangle$ can be determined by solving this eigenvalue Eq. 10. However, this is written on a much larger basis than the QRPA eigenvalue, and the task of diagonalizing the Hamiltonian in Eq. 10 is too demanding from a computational viewpoint, in particular for heavy nuclei. Therefore, we use projection techniques in order to obtain an equation expressed in the two-quasi-particle basis only.

If we project the full QPVC equation in the subspace spanned by the simple two quasi-particle excitations, that is, the QRPA space, and use the basis of the QRPA eigenstates, we obtain

$$\begin{pmatrix} \mathcal{D} + \mathcal{A}^{(1)}_{\pi\nu,\pi'\nu'}(E) & \mathcal{A}^{(2)}_{\pi\nu,\pi'\nu'}(E) \\ -\mathcal{A}^{(3)}_{\pi\nu,\pi'\nu'}(-E) & -\mathcal{D} - \mathcal{A}^{(4)}_{\pi\nu,\pi'\nu'}(-E) \end{pmatrix} \begin{pmatrix} \mathcal{X}_{\pi\nu} \\ \mathcal{Y}_{\pi\nu} \end{pmatrix} = E \begin{pmatrix} \mathcal{X}_{\pi\nu} \\ \mathcal{Y}_{\pi\nu} \end{pmatrix}. \quad (11)$$

Due to the projection, the matrix becomes energy-dependent and complex (this means that now, $E = \hbar\Omega - i\frac{\Gamma}{2}$). The matrix $\mathcal{D}$ is the diagonal matrix that contains the QRPA eigenvalues. The matrices $\mathcal{A}_i$ are associated with the coupling of the QRPA states with the doorway states. Accordingly, they are linear combinations of the QRPA amplitudes X and Y with the matrix elements of the operator $W^\downarrow$ [see Eqs 5–8 presented by Niu et al. (2016)], and $W^\downarrow$ is the operator that defines the coupling between two quasi-particle states and doorway states. Its matrix elements are associated with the self-energy of the two quasi-particle states. The diagrams corresponding to this self-energy are displayed in Figure 2.

With the eigenvalues and eigenvectors, which are the solutions to Eq. 11, we can determine either the strength associated with a general operator or the beta-decay half-lives. The strength function associated with QRPA + QPVC is given as

$$S(E) = -\frac{1}{\pi} \mathrm{Im} \sum_N \frac{\langle 0|\widehat{O}|N\rangle^2}{E - \Omega_N + i\left(\frac{\Gamma_N}{2} + \varepsilon\right)}. \quad (12)$$

As briefly mentioned above, the fine structure of the strength distributions, the widths of giant resonances (GRs), and their decay properties are not well described by QRPA because of the lack of coupling with more complex configurations than the two quasi-particles. The particle–vibration coupling (PVC) effects have been proven to be very effective in reproducing the missing physics mentioned above, so that the strength function (Eq. 12) agrees

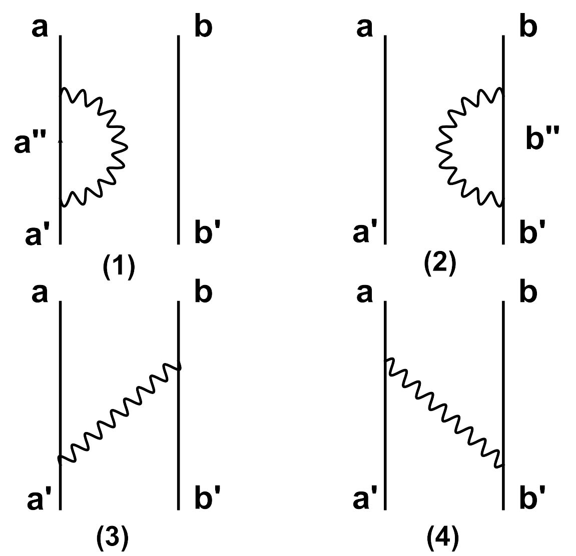

FIGURE 2
Diagrammatic representation of the four terms whose sum gives the matrix element $W^\downarrow$. Full (wavy) lines correspond to quasi-particles (phonons). Here, we keep a more general notation $a, b\ldots$ for the quasi-particles instead of labeling them either as protons or neutrons as in the main text [figure taken from the study by Niu et al. (2016)].

well with experiment. These particle–vibration coupling effects have been included in a self-consistent way, based on nonrelativistic EDFs, first without pairing effects (Colò et al., 1994; Niu et al., 2012) and then in their version with pairing included (Niu et al., 2016; Li et al., 2023). (Q)PVC effects have also been included on top of the covariant version of DFT (Litvinova et al., 2007; Litvinova et al., 2008). In this work, we review the applications of (Q)RPA + (Q)PVC to the study of β-decay (Niu et al., 2015; Niu et al., 2018).

Next, we also mention the second RPA (SRPA). The structure of the model has some analogy with RPA + PVC, but the "doorway states," instead of being particle–hole plus an extra phonon, are two particle–two holes (2p–2h).

4 Results

The first set of results is shown in Figure 3. In this figure, the RPA and RPA + PVC results are compared with the experiment. We chose different Skyrme EDFs: as said, the calculations contain no adjustable parameter, but the results are sensitive to the choice of the functional. There is a general trend that is almost independent of the chosen EDF: the β-decay half-lives are very significantly reduced by PVC effects (note the logarithmic scale), and RPA + PVC improves the results by bringing them closer to the experimental data. SkX is the only exception, but this functional has also been fit to single-particle energies in some of these nuclei. SLy5 is also a "gray" case, but in all other cases, the effect is clear.

In the figure, the arrows indicate the large or infinite half-lives (larger than 10^6 in the case of this figure). RPA + PVC solves, at least in many, if not all, cases, the puzzle of the very large half-lives. We qualitatively explained this feature in our discussion of Figure 1. In the paradigmatic case of ^{132}Sn, in which we previously mentioned

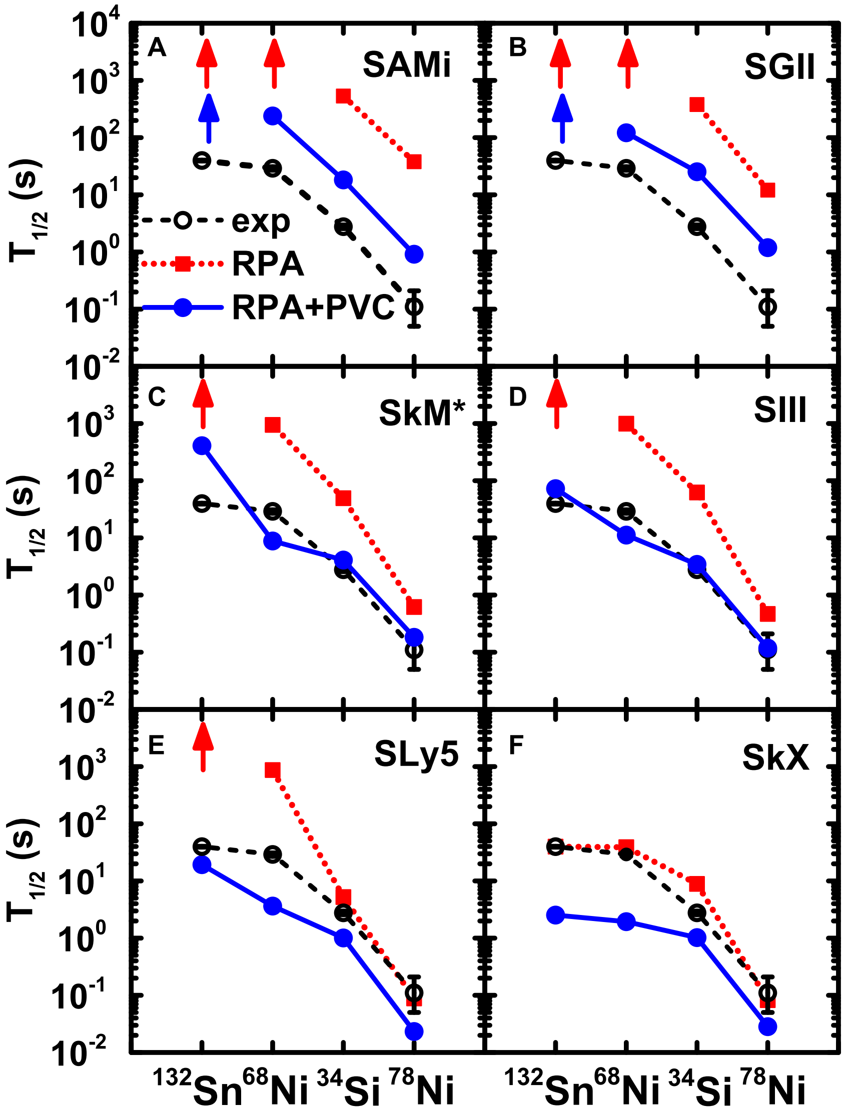

FIGURE 3
β-decay half-lives in the case of ^{132}Sn, ^{68}Ni, ^{34}Si, and ^{78}Ni. The RPA and RPA + PVC results are compared with the experimental half-lives, taken from http://www.nndc.bnl.gov [figure taken from the study by Niu et al. (2015)]. **(A–F)** include results for the same nuclei, yet obtained with different Skyrme EDFs.

that two states are experimentally observed in the Q_β window, with the interaction SkM $*$, there is no state within that window at the level of RPA so that the half-life is infinite. When we include PVC, one state is brought inside the window, which is the key point. The self-energy effects depicted in Figure 2 are mainly attractive at low energy because the doorway states lie, on average, at higher energy, and the energy denominators of those Feynman diagrams are negative. More examples are (briefly) discussed by Niu et al. (2015).

When the RPA "puzzle" of very large half-lives has become apparent, different solutions have been proposed. One possibility is to invoke an attractive $T = 0$ pairing force. This is active when the usual $T = 1$ pairing is non-vanishing, as discussed in the next section, and cannot play a role in the nuclei that we discussed so far if they are magic, i.e., they have closed shells. The role of pairing is discussed in detail in the next section. Other authors have emphasized the role of the tensor force in β-decay (Minato and Bai, 2013). The tensor force strongly affects both single-particle states (in particular, their spin–orbit splittings) and collective spin–flip excitations, as is natural; it is natural that it also affects β-decay. However, we still do not have a reliable, universal parametrization for the tensor force. A narrow interval for the tensor force parameters has been suggested by Bai et al. (2011), and new results on the M1 excitations seem to question this conclusion (Sun et al., 2024).

In summary, our results hint that PVC effects are genuine many-body effects that should be included in β-decay EDF-based calculations. One can aim at improving the EDFs themselves, either with a better fitting procedure or by including tensor terms; however, this should be done in addition to, not as an alternative to, including many-body effects. This is also the conclusion of Liu et al. (2024), which we discuss further in the following sections. Last but not least, our conclusion is supported by the SRPA calculations of β-decay half-lives that have been reported by Yang et al. (2023).

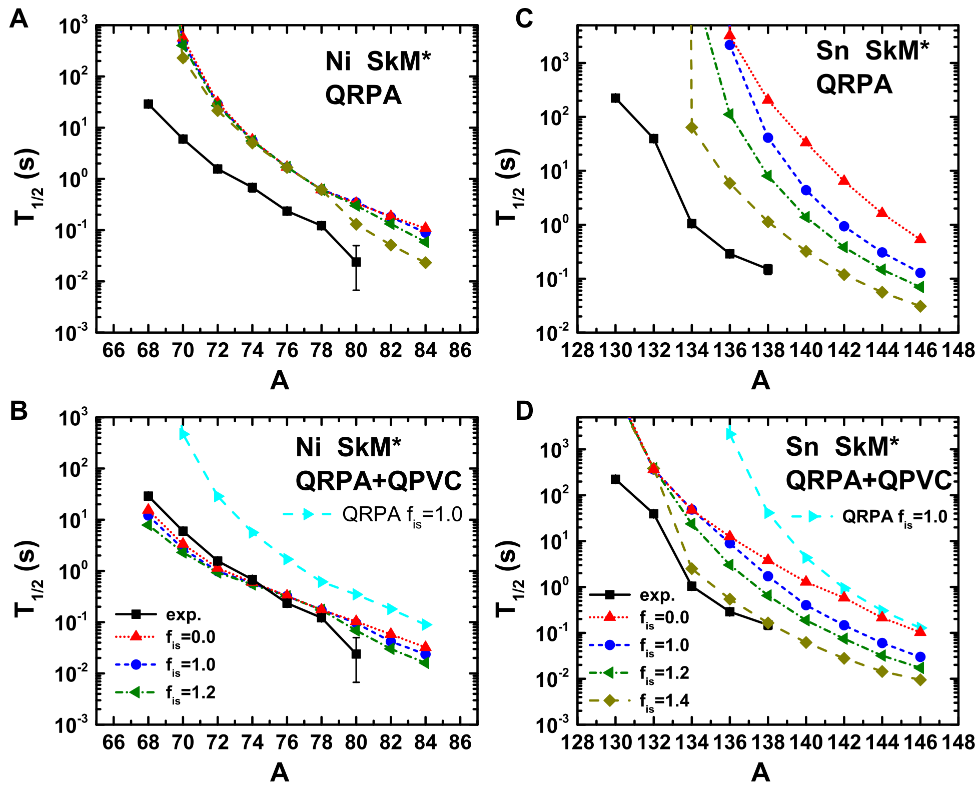

FIGURE 4
β-decay half-lives in the case of Ni and Sn isotopes. The theoretical results are compared with experimental data obtained by Audi et al. (2017) [figure taken from the study by Niu et al. (2018)] [the figure has been modified]. **(A–D)** display results for the Ni (Sn) isotopes, obtained either within QRPA or QRPA+QPVC.

5 Isoscalar pairing

Although the usual neutron–neutron or proton–proton, $T = 1$, pairing is rather well-known and gives rise to observable phenomena that can be associated with the superfluid character of part of the nucleons in a nucleus, the proton–neutron pairing, and, in particular, its isoscalar $T = 0$ component, is still elusive [Sagawa et al. (2016) provided a recent review]. There is no evidence, to date, of a proton–neutron superfluid. However, the $T = 0$ pairing interaction has $S = 1$ character in the $L = 0$ channel and can be active, or even strong, when protons and neutrons occupy excited single-particle states that can be coupled to $L = 0, S = 1$, like in the GT case. This explains why isoscalar pairing is relevant for β-decay studies; however, as already mentioned, this is possible only in non-magic nuclei.

The isoscalar pairing strength cannot be unambiguously fixed, and in all calculations, it is more or less left as a free parameter. Often, a parameter g is included that represents the ratio between the isoscalar and isovector pairing strengths, the latter being a more controlled quantity that can be fit using the pairing gaps or similar related observables. Setting $g = 0$ is legitimate, while a very large value of g looks unnatural. Several lines of empirical evidence (Sagawa et al., 2016) suggest a value of g of the order of 1 but somewhat larger ($g \approx 1.5$). We explored the sensitivity of β-decay half-lives to the choice of g in Niu et al. (2018).

The main motivation of the work by Niu et al. (2018) was to confirm that the conclusion reached for magic nuclei, i.e., that PVC effects play a substantial role in β-decay, also holds when one investigates open-shell nuclei and RPA + PVC becomes QRPA + QPVC. We picked up the SkM* EDF that is most successful for magic nuclei (cf. the previous section). We added, in the pairing sector, a zero-range, density-dependent pairing interaction. After fitting its isovector component in order to reproduce the pairing gaps Δ, we allowed slight variations in such strength through a renormalization parameter f_{IV}, and we also introduced a similar parameter f_{IS} for isoscalar pairing. In the language of the previous paragraph, $g \equiv \frac{f_{IS}}{f_{IV}}$.

The effect of the isovector pairing on the β-decay half-lives is not large at the QRPA level. This is the result of two competing effects. By increasing the strength f_{IV}, the gaps become larger and the energy of the two quasi-particle configurations increases (which increases their half-life); at the same time, the occupation of the levels is more smeared out; that is, low-lying levels become emptier, and high-lying levels become more occupied (which reduces the half-life). Interestingly, the effect of isovector pairing becomes weaker at the level of QRPA + QPVC. To obtain the results given in Figure 4, we then fixed $f_{IV} = 1$ so that $f_{IS} = g$.

We confirmed in our work that isoscalar pairing is more important. As mentioned, we expect that isoscalar pairing has effects when the proton and neutron levels with relative $L = 0, S = 1$ are partially filled. In this respect, its impact depends on the specific shell structure(s). Figure 4 shows that isoscalar pairing plays a role in the Sn isotopes above ^{132}Sn (Figures 4C, D), while it is much less important in the Ni isotopes (Figures 4A, B). In ^{134}Sn and the next isotopes, for example, the transition between the neutron $h_{11/2}$ state and the proton $h_{11/2}$ state starts to play a role (cf., again, the left panel of Figure 1). This is pushed at lower energy and attracts strength from other GT transitions precisely because of the matrix elements of the isoscalar pairing force. The overall effect is a decrease in the half-lives of Sn isotopes in that region, and as the matrix elements are weighted by f_{IS}, we explain the behavior in the right panels of Figure 4. A more detailed discussion is presented by Niu et al. (2018).

In summary, the QPVC effects and the isoscalar pairing interaction contribute to a decrease in the β-decay half-lives. IS pairing is already present at the QRPA level. However, including only IS pairing would not be sufficient to reproduce the experimental half-lives given in Figure 4. Although QPVC effects are non-negligible in all the nuclei studied, the impact of the isoscalar pairing depends more on the specific levels involved in the GT transitions and, in particular, on their partial occupations. Moreover, the former is a many-body effect, while the latter is sensitive to the strength of the isoscalar pairing interaction. It is quite encouraging, although in the case in which the sensitivity to that interaction is stronger (the Sn isotopes above the $N = 82$ shell closure), the value of f_{IS} that allows reproducing experimental data ($f_{IS} = 1.4$) is similar to previous estimates.

6 Deformation, large-scale calculations, and future prospects

Recently, Liu et al. (2024) also advocated that QPVC effects and isoscalar pairing are indeed relevant. However, it is argued that one can draw firmer quantitative conclusions and build a model with real predictive power by considering a larger sample than spherical nuclei. The deformed charge-exchange QRPA was developed by Sarriguren et al. (1998); Sarriguren et al. (1999); Sarriguren et al. (2001) using the BCS scheme. These studies, as well as more recent works, clarified the sensitivity of β-decay to deformation. Liu et al. (2024) implemented axially deformed QRPA on top of HFB. Moreover, the QPVC is considered based on the finite amplitude method (FAM). QPVC is in its matrix formulation, as explained in the previous sections, and has been deemed to be computationally too expensive to be systematically applied throughout the periodic table.

Table 1 in the study by Liu et al. (2024) confirms our main statement that QPVC is a very crucial factor, reducing half-lives and aligning them closer to the experimental data. This is confirmed by a different group that employed a quite different implementation and considered axially deformed nuclei instead of spherical nuclei. The scope of the research reported by Liu et al. (2024) is quite broad and ambitious: the idea is to make the approach even more computationally effective, fit a new EDF at the QPVC level, and test the model on large-scale calculations. It remains an open question whether the assumption of axial symmetry has to be abandoned at some stage.

The conclusion and perspectives presented by Liu et al. (2024) raise interesting questions that lie at the very heart of the nuclear many-body problem. Although QRPA + QPVC can certainly catch the most important correlations that affect low-lying nuclear excitations, we still do not know its limitations in a quantitative way. To date, the parameters of an EDF have not been fit at the level of QPVC. Ultimately, we share the opinion expressed by Liu et al. (2024), that is, that if one does so, the scheme goes in the direction of an *ab initio* solution to the many-body problem. The added value of β-decay in this game is two-fold: β-decay half-lives are very sensitive to the low-lying spectra and also to specific terms of the nuclear Hamiltonian or EDF (spin–isospin terms and isoscalar pairing). In this respect, experimental progress has to be encouraged and may yield new results.

Author contributions

GC: conceptualization, data curation, methodology, supervision, writing–original draft, and writing–review and editing. YN: conceptualization, data curation, methodology, supervision, writing–original draft, and writing–review and editing.

Funding

The author(s) declare that financial support was received for the research, authorship, and/or publication of this article. YN acknowledges funding from the National Key Research and Development (R&D) Program under grant no. 2021YFA1601500 and the Natural Science Foundation of China under grant no. 12075104. GC acknowledges funding from the APC fund of the University of Milan, and from the European Union's Horizon Europe research and innovation programme under grant agreement no. 101057511.

Conflict of interest

The authors declare that the research was conducted in the absence of any commercial or financial relationships that could be construed as a potential conflict of interest.

Publisher's note

References

Audi, G., Kondev, F. G., Meng, W., Huang, W. J., and Naimi, S. (2017). The nubase2016 evaluation of nuclear properties. *Chin. Phys. C* 41, 030001. doi:10.1088/1674-1137/41/3/030001

Bai, C. L., Zhang, H. Q., Sagawa, H., Zhang, X. Z., Colò, G., and Xu, F. R. (2011). Spin-isospin excitations as quantitative constraints for the tensor force. *Phys. Rev. C* 83, 054316. doi:10.1103/PhysRevC.83.054316

Borzov, I. (2006). Beta-decay rates. *Nucl. Phys. A* 777, 645–675. doi:10.1016/j.nuclphysa.2005.05.147

Colò, G. (2020). *Nuclear density functional theory (DFT)*. Singapore: Springer Nature Singapore, 1–30. doi:10.1007/978-981-15-8818-1_14-1

Colò, G., Cao, L., Van Giai, N., and Capelli, L. (2013). Self-consistent rpa calculations with skyrme-type interactions: the skyrme_rpa program. *Comput. Phys. Commun.* 184, 142–161. doi:10.1016/j.cpc.2012.07.016

Colò, G., Van Giai, N., Bortignon, P. F., and Broglia, R. A. (1994). Escape and spreading properties of charge-exchange resonances in ^{208}Bi. *Phys. Rev. C* 50, 1496–1508. doi:10.1103/PhysRevC.50.1496

Dolinski, M. J., Poon, A. W., and Rodejohann, W. (2019). Neutrinoless double-beta decay: status and prospects. *Annu. Rev. Nucl. Part. Sci.* 69, 219–251. doi:10.1146/annurev-nucl-101918-023407

Fang, D.-L., Brown, B. A., and Suzuki, T. (2013). Investigating β-decay properties of spherical nuclei along the possible *r*-process path. *Phys. Rev. C* 88, 034304. doi:10.1103/physrevc.88.034304

Fracasso, S., and Colò, G. (2007). Spin-isospin nuclear response using the existing microscopic skyrme functionals. *Phys. Rev. C* 76, 044307. doi:10.1103/PhysRevC.76.044307

Gorchtein, M., and Seng, C.-Y. (2024). Superallowed nuclear beta decays and precision tests of the standard model. *Annu. Rev. Nucl. Part. Sci.* doi:10.1146/annurev-nucl-102622-020726

Gysbers, P., Hagen, G., Holt, J. D., Jansen, G. R., Morris, T. D., Navrátil, P., et al. (2019). Discrepancy between experimental and theoretical β-decay rates resolved from first principles. *Nat. Phys.* 15, 428–431. doi:10.1038/s41567-019-0450-7

Hayen, L. (2024). [Dataset] *Opportunities and open questions in modern β-decay*.

Homma, H., Bender, E., Hirsch, M., Muto, K., Klapdor-Kleingrothaus, H. V., and Oda, T. (1996). Systematic study of nuclear β-decay. *Phys. Rev. C* 54, 2972–2985. doi:10.1103/physrevc.54.2972

Janka, H.-T., Melson, T., and Summa, A. (2016). Physics of core-collapse supernovae in three dimensions: a sneak preview. *Annu. Rev. Nucl. Part. Sci.* 66, 341–375. doi:10.1146/annurev-nucl-102115-044747

Kajino, T., Aoki, W., Balantekin, A., Diehl, R., Famiano, M., and Mathews, G. (2019). Current status of *r*-process nucleosynthesis. *Prog. Part. Nucl. Phys.* 107, 109–166. doi:10.1016/j.ppnp.2019.02.008

Langanke, K., and Martínez-Pinedo, G. (2003). Nuclear weak-interaction processes in stars. *Rev. Mod. Phys.* 75, 819–862. doi:10.1103/RevModPhys.75.819

Li, Z. Z., Niu, Y. F., and Colò, G. (2023). Toward a unified description of isoscalar giant monopole resonances in a self-consistent quasiparticle-vibration coupling approach. *Phys. Rev. Lett.* 131, 082501. doi:10.1103/PhysRevLett.131.082501

Litvinova, E., Ring, P., and Tselyaev, V. (2008). Relativistic quasiparticle time blocking approximation: dipole response of open-shell nuclei. *Phys. Rev. C* 78, 014312. doi:10.1103/PhysRevC.78.014312

Litvinova, E., Ring, P., and Vretenar, D. (2007). Relativistic rpa plus phonon-coupling analysis of pygmy dipole resonances. *Phys. Lett. B* 647, 111–117. doi:10.1016/j.physletb.2007.01.056

Liu, Q., Engel, J., Hinohara, N., and Kortelainen, M. (2024). Effects of quasiparticle-vibration coupling on gamow-teller strength and β-decay with the skyrme proton-neutron finite-amplitude method. *Phys. Rev. C* 109, 044308. doi:10.1103/PhysRevC.109.044308

Mach, H., Jerrestam, D., Fogelberg, B., Hellström, M., Omtvedt, J. P., Erokhina, K. I., et al. (1995). Structure of the p-h nucleus ^{132}Sb. *Phys. Rev. C* 51, 500–508. doi:10.1103/PhysRevC.51.500

Marketin, T., Litvinova, E., Vretenar, D., and Ring, P. (2012). Fragmentation of spin-dipole strength in 90zr and 208pb. *Phys. Lett. B* 706, 477–481. doi:10.1016/j.physletb.2011.11.050

Minato, F., and Bai, C. L. (2013). Impact of tensor force on β- decay of magic and semimagic nuclei. *Phys. Rev. Lett.* 110, 122501. doi:10.1103/PhysRevLett.110.122501

Möller, P., Nix, J. R., and Kratz, K. L. (1997). Nuclear properties for astrophysical and radioactive-ion-beam application. *At. Data Nucl. Data Tables* 66, 131–343. doi:10.1006/adnd.1997.0746

Mustonen, M. T., and Engel, J. (2016). Global description of β- decay in even-even nuclei with the axially-deformed skyrme finite-amplitude method. *Phys. Rev. C* 93, 014304. doi:10.1103/PhysRevC.93.014304

Ney, E. M., Engel, J., Li, T., and Schunck, N. (2020). Global description of β- decay with the axially deformed skyrme finite-amplitude method: extension to odd-mass and odd-odd nuclei. *Phys. Rev. C* 102, 034326. doi:10.1103/PhysRevC.102.034326

Nikšić, T., Marketin, T., Vretenar, D., Paar, N., and Ring, P. (2005). β-decay rates of *r*-process nuclei in the relativistic quasiparticle random phase approximation. *Phys. Rev. C* 71, 014308. doi:10.1103/PhysRevC.71.014308

Niu, Y., Niu, Z., Colò, G., and Vigezzi, E. (2018). Interplay of quasiparticle-vibration coupling and pairing correlations on β-decay half-lives. *Phys. Lett. B* 780, 325–331. doi:10.1016/j.physletb.2018.02.061

Niu, Y. F., Colò, G., Brenna, M., Bortignon, P. F., and Meng, J. (2012). Gamow-teller response within skyrme random-phase approximation plus particle-vibration coupling. *Phys. Rev. C* 85, 034314. doi:10.1103/PhysRevC.85.034314

Niu, Y. F., Colò, G., Vigezzi, E., Bai, C. L., and Sagawa, H. (2016). Quasiparticle random-phase approximation with quasiparticle-vibration coupling: application to the gamow-teller response of the superfluid nucleus ^{120}Sn. *Phys. Rev. C* 94, 064328. doi:10.1103/PhysRevC.94.064328

Niu, Y. F., Niu, Z. M., Colò, G., and Vigezzi, E. (2015). Particle-vibration coupling effect on the β- decay of magic nuclei. *Phys. Rev. Lett.* 114, 142501. doi:10.1103/PhysRevLett.114.142501

Niu, Z. M., Niu, Y. F., Liang, H. Z., Long, W. H., Nikšić, T., Vretenar, D., et al. (2013). β-decay half-lives of neutron-rich nuclei and matter flow in the *r*-process. *Phys. Lett. B* 723, 172–176. doi:10.1016/j.physletb.2013.04.048

Qian, Y.-Z., and Wasserburg, G. (2007). Where, oh where has the *r*-process gone? *Phys. Rep.* 442, 237–268. doi:10.1016/j.physrep.2007.02.006

Rubio, B., Gelletly, W., and Naviliat-Cuncic, O. (2020). *Beta decay: probe for nuclear structure and the weak interaction*. Singapore: Springer Nature Singapore, 1–49. doi:10.1007/978-981-15-8818-1_43-1

Sagawa, H., Bai, C. L., and Colò, G. (2016). Isovector spin-singlet (t = 1, s = 0) and isoscalar spin-triplet (t = 0, s = 1) pairing interactions and spin-isospin response. *Phys. Scr.* 91, 083011. doi:10.1088/0031-8949/91/8/083011

Sarriguren, P., Moya de Guerra, E., and Escuderos, A. (1999). Shapes and β-decay in proton rich ge, se, kr and sr isotopes. *Nucl. Phys. A* 658, 13–44. doi:10.1016/S0375-9474(99)00346-2

Sarriguren, P., Moya de Guerra, E., and Escuderos, A. (2001). Spin–isospin excitations and β^+/ec half-lives of medium-mass deformed nuclei. *Nucl. Phys. A* 691, 631–648. doi:10.1016/S0375-9474(01)00565-6

Sarriguren, P., Moya de Guerra, E., Escuderos, A., and Carrizo, A. (1998). β-decay and shape isomerism in ^{74}kr. *Nucl. Phys. A* 635, 55–85. doi:10.1016/S0375-9474(98)00158-4

Schunck, N. (2019). *Energy density functional methods for atomic nuclei* (Bristol: IoP Publishing).

Shafer, T., Engel, J., Fröhlich, C., McLaughlin, G. C., Mumpower, M., and Surman, R. (2016). β- decay of deformed *r*-process nuclei near $a = 80$ and $a = 160$, including odd-a and odd-odd nuclei, with the skyrme finite-amplitude method. *Phys. Rev. C* 94, 055802. doi:10.1103/PhysRevC.94.055802

Sun, S., Cao, L.-G., Zhang, F.-S., Sagawa, H., and Colò, G. (2024). Microscopic study of $m1$ resonances in sn isotopes. *Phys. Rev. C* 109, 014321. doi:10.1103/PhysRevC.109.014321

Yang, M. J., Sagawa, H., Bai, C. L., and Zhang, H. Q. (2023). Effects of two-particle–two-hole configurations and tensor force on β- decay of magic nuclei. *Phys. Rev. C* 107, 014325. doi:10.1103/PhysRevC.107.014325

Yannouleas, C. (1987). Zero-temperature second random phase approximation and its formal properties. *Phys. Rev. C* 35, 1159–1161. doi:10.1103/PhysRevC.35.1159

Yasuda, J., Sasano, M., Zegers, R. G. T., Baba, H., Bazin, D., Chao, W., et al. (2018). Extraction of the landau-migdal parameter from the gamow-teller giant resonance in ^{132}Sn. *Phys. Rev. Lett.* 121, 132501. doi:10.1103/PhysRevLett.121.132501